Available online at www.sciencedirect.com
SCIENCE DIRECT®
Polymer 44 (2003) 5789–5796
polymer
www.elsevier.com/locate/polymer

Structure alterations of perfluorinated sulfocationic membranes under the action of ethylene glycol (SAXS and WAXS studies)

A.V. Krivandin[a,*], A.B. Solov'eva[b], N.N. Glagolev[b], O.V. Shatalova[a], S.L. Kotova[b]

[a]*Institute of Biochemical Physics, Russian Academy of Sciences, Kosygin str. 4, 119991 Moscow, Russian Federation*
[b]*Institute of Chemical Physics, Russian Academy of Sciences, Kosygin str. 4, 119991 Moscow, Russian Federation*

Received 13 March 2003; received in revised form 2 June 2003; accepted 27 June 2003

Abstract

Small-angle X-ray scattering and wide-angle X-ray scattering studies were carried out for perfluorinated sulfocationic membranes MF-4SK (membranes of a Nafion type) in the normal 'as-manufactured' state and soaked in ethylene glycol at 110 °C and subsequently washed with water. It was shown that such a treatment of MF-4SK membranes resulted in alterations of their nanostructure and these alterations were stable for a long time. On the basis of the paracrystalline layered model of the perfluorinated membrane nanostructure these structure alterations were interpreted as an increase in the thickness of the liquid layers (ionic channels) separating clusters of ionomer groups in MF-4SK membranes. The importance of these structure alterations was confirmed by the twofold growth of the quantum yield of anthracene photo-oxidation catalyzed by tetraphenylporphyrin (TPP) immobilized on MF-4SK membranes treated with ethylene glycol.

Keywords: Perfluorinated sulfocationic membrane; Ethylene glycol; Structure alteration

1. Introduction

Perfluorinated sulfocationic membranes are derived from copolymers of tetrafluoroethylene and perfluorovinyl ether terminating in a sulfo group and have the following structural formula

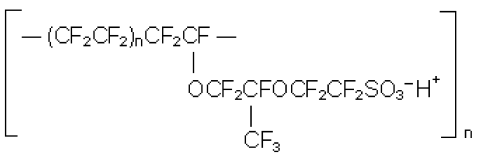

Such membranes are widely used in electrochemical technologies including chlor-alkali production and proton exchange membrane fuel cells [1–3]. They have also appeared to be a promising material for the developments of novel sensors, electrochromic or photoconversion devices and heterogeneous electrocatalytic and photocatalytic systems where they are often used as matrices for the immobilization of reactive low molecular weight compounds or enzymes [4–15].

The structure of perfluorinated ionomer membranes was intensively studied with various techniques including X-ray and neutron diffraction methods [16–33]. The main structural feature of these membranes is microphase separation associated with clustering of ionomer groups. However, the detailed structure of these membranes was not unequivocally determined up to now [24,28,31–33].

One of the methods of modification of perfluorinated membranes properties which may be essential for their technological applications is the treatment of these membranes with alcohol or glycol resulting in additional swelling of these membranes. In order to get an insight into the molecular mechanisms of this process we have carried out the small-angle X-ray scattering (SAXS) and wide-angle X-ray scattering (WAXS) studies of these membranes before and after swelling with ethylene glycol. We have also analyzed some chemical properties of these membranes before and after such a swelling and correlated the modification of these properties with the membrane structure alterations revealed.

* Corresponding author. Tel.: +7-95-9397324; fax: +7-95-1374101.
E-mail address: krivandin@sky.chph.ras.ru (A.V. Krivandin).

0032-3861/03/$ - see front matter © 2003 Elsevier Ltd. All rights reserved.
doi:10.1016/S0032-3861(03)00588-3

2. Experimental

The perfluorinated sulfocationic membranes with the trademark 'MF-4SK' were obtained from the 'Plastpolymer' company (St. Petersburg, Russia) in the H^+-ionic form in the wet state (swollen in distilled water). These membranes were prepared by the extrusion method, had the nominal thickness of 120 μm and the exchange capacity of 0.87 mg Equiv. per gram that corresponds to the equivalent weight (i.e. the weight of polymer which will neutralize 1 Equiv. of a base) of 1150 g/Equiv. For the treatment with ethylene glycol MF-4SK membranes were soaked in ethylene glycol at 110 °C for a predefined period of time and then washed thoroughly with distilled water. Membranes in the air-dried state (dry membranes) were obtained by drying in the room ambient conditions for 24 h. The water content in membranes was measured gravimetrically as the weight difference between membranes in the wet and in the dry states. For immobilization of TPP membranes were stored in a 10^{-3} M solution of TPP ('Merck', USA) in chloroform for 24 h and then washed with pure chloroform in a Soxlet apparatus.

Photo-oxidation of anthracene (high purity grade) was carried out in 7×10^{-4} M chloroform solution with oxygen of the air in the presence of MF-4SK membranes with immobilized TPP. The TPP content in MF-4SK membranes was $(3-10) \times 10^{-8}$ M/cm^2. The solution was illuminated with a filtered light of a mercury lamp ($\lambda > 580$ nm). The efficiency of singlet oxygen generation was estimated as the quantum yield $\Phi(AO_2)$ of photosensitized oxidation of anthracene. The $\Phi(AO_2)$ values were calculated as the ratio of the number of oxidized anthracene molecules (in the linear part of the kinetic curve) to the number of the light quanta absorbed by the immobilized TPP. The number of oxidized anthracene molecules in the solution was determined by the height of anthracene absorption bands in the range of 300–400 nm. Electron absorption spectra were measured with a 'Specord M-40' spectrophotometer.

The SAXS and WAXS measurements were performed for MF-4SK membranes in the wet and in the air-dried states in transmission geometry using the X-ray diffractometer of a local design. In the course of the X-ray exposure membranes were kept in the sealed cell preventing their dehydration. The X-ray radiation from the fine focus Cu X-ray tube run at 30 kV/30 mA was Ni-filtered and line-focused with the glass mirror collimator of Franks type [34]. X-ray scattering patterns were recorded with the gas-filled (85% Xe, 15% Me) one-dimensional position-sensitive detector with delay line readout constructed in JINR [35]. The sample-to-detector distance was 415 mm for SAXS and 140 mm for WAXS measurements. Experimental curves were corrected for the background scattering, desmeared by the method [36] and plotted as the functions of $S = (2 \sin \theta)/\lambda$, where λ is Cu K_α-wavelength (0.1542 nm) and θ is a half of the scattering angle.

As a test for the membranes structural isotropy two-dimensional WAXS patterns were recorded in the X-ray camera with a pinhole collimation and a flat X-ray film. No preferred orientation (texture) in the plane of these membranes was revealed by this method.

3. Results

The SAXS and WAXS patterns for the wet MF-4SK membranes (membranes swollen in water) are shown in Figs. 1 and 2. In order to depict the inner part of the SAXS curve more clearly the S-axis in Fig. 1 is given on a logarithmic scale. The SAXS pattern for MF-4SK membranes exhibits two maxima at $S \approx 0.055$ and 0.2 nm^{-1} corresponding to the Bragg distances $d = (S)^{-1}$ of approximately 18 and 5 nm. Similar small-angle maxima (but sometimes at different d values) were observed for perfluorinated sulfocationic membranes in the earlier small-angle neutron scattering [16,27,31] and SAXS [17–24,27,31] studies. The first maximum (18 nm in this study) may be attributed (as in the case of many other semicrystalline polymers) to the scattering by alternating crystalline and amorphous regions. The second maximum (5 nm) is associated with the existence of clusters of ionomer groups (ionic clusters) in perfluorinated sulfocationic membranes [16–18]. The low intensity of the first maximum corresponds to the low crystallinity of perfluorinated membranes with the equivalent weight of 1150 g/Equiv. studied in this work. It was shown in the earlier WAXS studies that crystallinity of perfluorinated membranes grew with the increase in the equivalent weight [17,18].

The WAXS pattern for MF-4SK membranes comprises a broad diffraction maximum centered at $S \approx 1.9$ nm^{-1} (Fig. 2). This pattern is very similar to the WAXS patterns for Nafion membranes with the analogous equivalent weight [17,18,23].

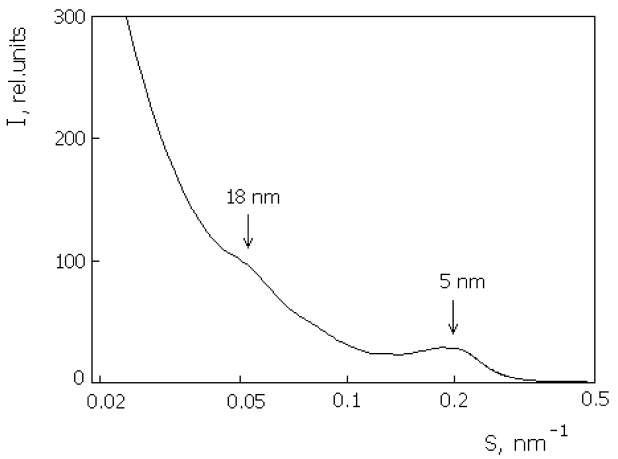

Fig. 1. SAXS pattern for MF-4SK wet membranes. The S-axis is on a logarithmic scale. The arrows indicate the SAXS maxima corresponding to the Bragg distances of approximately 18 and 5 nm.

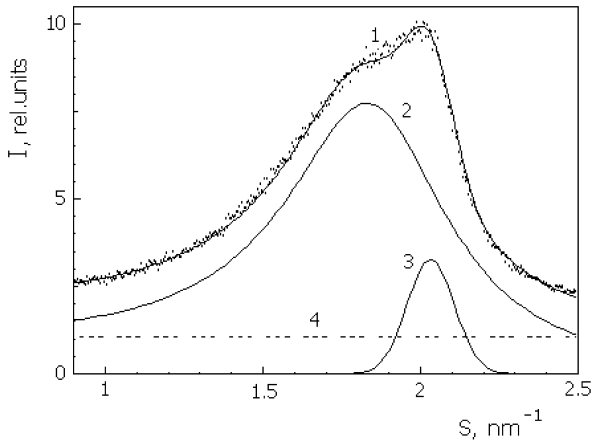

Fig. 2. WAXS pattern for MF-4SK wet membranes (dots) and its least-squares fit (1) by the sum of an amorphous peak (2), a crystalline peak (3) and a constant (4).

The diffraction maximum in Fig. 2 is markedly asymmetric. It can be decomposed into two diffraction peaks ascribed to the diffraction by amorphous and crystalline regions in perfluorinated membranes [17,18]. The best least-squares fit for the experimental intensity $I(S)$ we have got by decomposition according to the formula

$$I(S) = I_a(S) + I_c(S) + k \tag{1a}$$

$$I_a(S) = I_1(1 + ((S - S_1)/b_1)^2)^{-1} S^{-1} \tag{1b}$$

$$I_c(S) = I_2 \exp(-((S - S_2)/b_2)^2) \tag{1c}$$

with I_1, S_1, b_1, I_2, S_2, b_2, k as variables of such fit. The first item $I_a(S)$ in (1a) is a broad amorphous peak. It is given by the Cauchy distribution multiplied with S^{-1} to allow the asymmetry of this peak (the multiplier S^{-1} may be considered as the inverse Lorentz correction factor). The second peak $I_c(S)$ in (1a) is a rather sharp crystalline peak of the Gaussian form. Note that the polarization and absorption correction factors, as well as the influence of the Lorentz correction factor on the narrow crystalline peak $I_c(S)$, were neglected in this analysis because of their minor effect. The peaks $I_a(S)$ and $I_c(S)$ resulting from such a fit are shown in Fig. 2. The first broad asymmetric peak $I_a(S)$ has a maximum at $S = 1.85 \pm 0.02$ nm^{-1}. It accounts for the short-range order in perfluorinated membrane amorphous phase. The second rather sharp peak $I_c(S)$ centered at $S = 2.03 \pm 0.01$ nm^{-1} was indexed as the 100 reflection of the hexagonal crystalline lattice of a perfluorinated membrane [37].

The crystallinity of MF-4SK membranes we assessed as

$$C = \frac{\int I_c(S) S^2 \, dS}{\int [I_c(S) + I_a(S)] S^2 \, dS} \cdot 100\% \tag{2}$$

by integration over the interval from $S = 0.0$ to 4.0 nm^{-1} and found it to be about 10%. This value differs slightly from 12% [18] and 8% [20] reported earlier for perfluorinated sulfocationic membranes in H^+-ionic form with the analogous equivalent weight.

The effects of ethylene glycol treatment on the MF-4SK membrane structure are depicted by the WAXS and SAXS patterns in Figs. 3–7.

Ethylene glycol had only minor effect on WAXS patterns of MF-4SK membranes in the wet and in the dry states as shown in Figs. 3 and 4. Note that the patterns in Figs. 3 and 4 are extended to the higher S values than in Fig. 2. The main effect of ethylene glycol on the WAXS pattern for MF-4SK membranes in the wet state was some intensity elevation for $S > 2.5$ nm^{-1}. Water gives a diffraction halo in this S-range, and such an intensity elevation is very likely due to the higher water content in MF-4SK membranes treated with ethylene glycol as compared with the untreated membranes. This was confirmed by the comparative study of MF-4SK membranes treated and untreated with ethylene glycol when WAXS patterns were taken for membranes in the air-dried state (Fig. 4). The X-ray scattering for such membranes decreased for $S > 2.5$ nm^{-1} as compared with the wet membranes and was the same for membranes both treated and untreated with ethylene glycol.

The SAXS patterns for MF-4SK wet membranes before and after the treatment with ethylene glycol are shown in Figs. 5 and 6. Ethylene glycol almost did not influence the first maximum at $S \approx 0.055$ nm^{-1} (Fig. 5) and so it did not disturb the long-period structure in MF-4SK membranes. But the treatment with ethylene glycol increased significantly the intensity in the initial part of the SAXS pattern (Fig. 5).

According to the SAXS theory [38] such increase in the intensity may be caused by the increase in the quantity, size or electron density contrast of local heterogeneities (for example, small voids filled with water) in MF-4SK membranes after their treatment with ethylene glycol.

The most important effect of ethylene glycol on the MF-4SK membrane structure was revealed in the SAXS region of the second maximum at $S \approx 0.2$ nm^{-1} (Fig. 6). As a result of the MF-4SK membranes treatment with ethylene glycol this maximum significantly shifted to the smaller

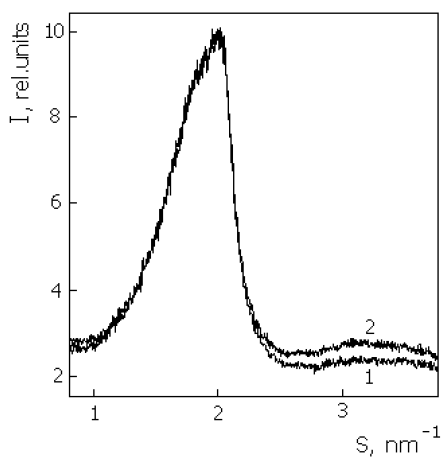

Fig. 3. WAXS patterns for MF-4SK wet membranes before (1) and after (2) the treatment with ethylene glycol for 9 min.

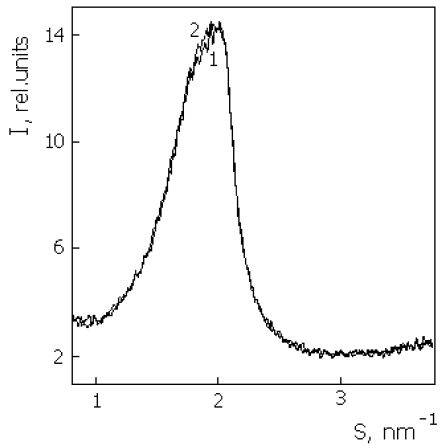

Fig. 4. WAXS patterns for MF-4SK air-dried membranes before (1) and after (2) the treatment with ethylene glycol for 9 min.

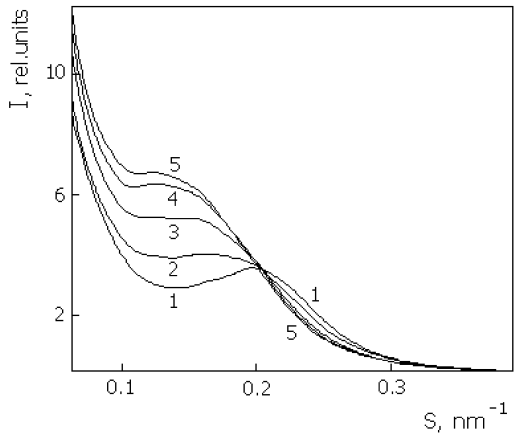

Fig. 6. SAXS patterns for MF-4SK wet membranes before (1) and after the treatment with ethylene glycol for 0.5 min (2), 2 min (3), 9 min (4) and 30 min (5).

angles. This implies essential alterations of membrane ordered nanostructure (i.e. the structure associated with the ionic clusters) under the action of ethylene glycol.

The structure alterations of MF-4SK membranes treated with ethylene glycol preserved at least partly after the membrane drying (Fig. 7). As in the earlier studies [17,18] the drying shifted the second SAXS maximum to higher S values (Fig. 7), but a clear difference in the SAXS patterns remained for the membranes treated with ethylene glycol and for the untreated membranes resembling the difference for these membranes in the wet state.

The structure alterations of MF-4SK membranes treated with ethylene glycol were stable at least for 5 months. This is illustrated by the SAXS patterns of one and the same membrane taken with the interval of 5 months after its prolonged soaking in water and repeated water changes (Fig. 8).

The time course of MF-4SK membrane structure alterations under the action of ethylene glycol was assessed with the analysis of the Bragg distance $d = (S_{max})^{-1}$ for the second SAXS maximum as a function of the duration of the membrane treatment with ethylene glycol. In order to determine these d values the SAXS patterns were decomposed by a least-squares fit into the Gaussian peak and the underlying diffusive scattering according to the formula

$$I(S) = I_{max} \exp(-\pi(S - S_{max})^2/\Delta_S^2) + a/(1 + (S/b)^2)^C \quad (3)$$

where I_{max}, S_{max}, Δ_S, a, b, c are variables of such a fit. An example of such a fit is shown in Fig. 9. The parameters of the Gaussian peaks (their height I_{max}, center S_{max}, and integral width Δ_S) found for all membranes by such fits and corresponding Bragg distances d are given in Table 1. The time course of d values (Table 1) shows that structure alterations of MF-4SK membrane under the action of ethylene glycol are rather fast. The main part of these alterations takes place in the first two minutes of membrane storage in ethylene glycol.

The time course of MF-4SK membrane structure alterations as depicted by d values (Table 1) correlates with the increase in the water content in MF-4SK membrane and the quantum yield of anthracene photo-oxidation catalyzed by tetraphenylporphyrin (TPP) immobilized on MF-4SK membrane (Table 2). Note that TPP immobiliz-

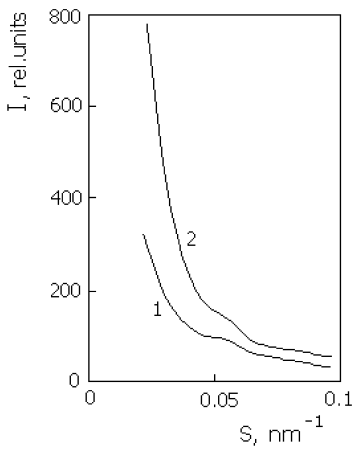

Fig. 5. SAXS patterns for MF-4SK wet membranes before (1) and after (2) the treatment with ethylene glycol for 9 min.

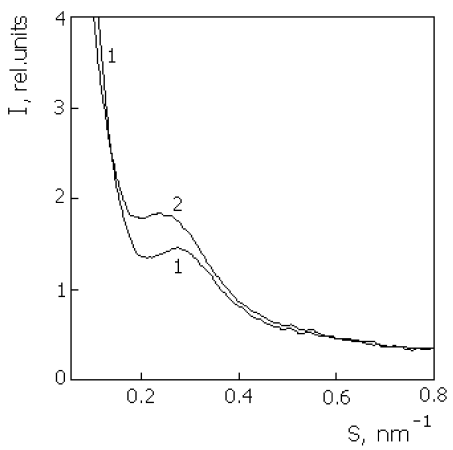

Fig. 7. SAXS patterns for MF-4SK air-dried membranes before (1) and after (2) the treatment with ethylene glycol for 9 min.

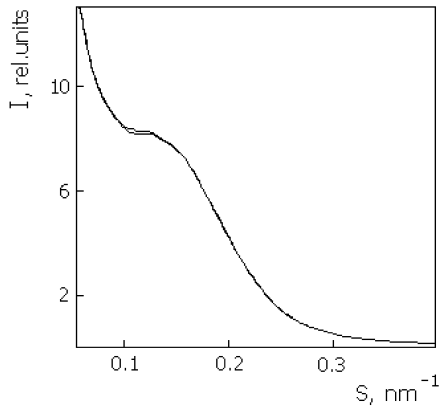

Fig. 8. Two SAXS patterns for MF-4SK wet membranes treated with ethylene glycol for 9 min. The patterns were taken with the interval of 5 months.

ation on MF-4SK membranes treated with ethylene glycol made it possible to obtain a much more effective photocatalytic system as compared with an untreated membrane. Very likely this is due to a higher TPP accessibility for a substrate in the treated membranes resulting from the structure alterations of these membranes.

The interpretation of the MF-4SK membrane structure alterations revealed depends on a nanostructure model of these membranes, i.e. a model of a spatial organization of ionic clusters accounting for the SAXS maximum at $S \approx 0.2\ \mathrm{nm}^{-1}$. Several very distinct structure models of these clusters have been proposed earlier [17–21,24–28,31–33,37]. We suppose the layered structure model to be the most probable as it accounts for the experimental SAXS data in the best way [20,21,39]. In this model bilayers of polytetrafluoroethylene backbone chains with copolymer perfluorovinyl ether side chains are separated by aqueous layers, copolymer side chains terminating by ionomer groups protrude into these aqueous layers and ionic clusters are formed by ionomer groups on each side of a polymeric bilayer (Fig. 10). For such a layered structure the SAXS

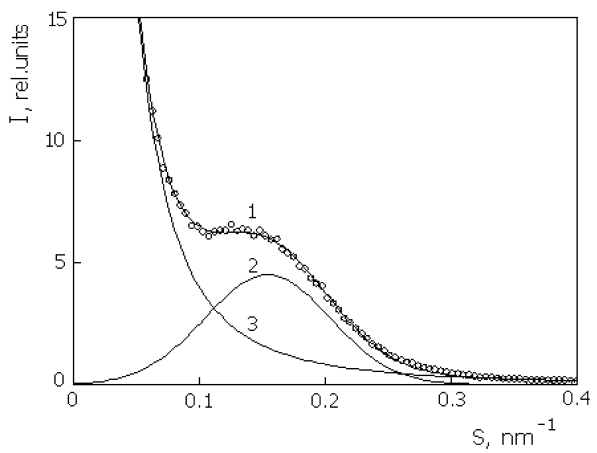

Fig. 9. SAXS pattern for MF-4SK wet membranes treated with ethylene glycol for 9 min (dots) and its least-squares fit (1) with the sum of a Gaussian peak (2) and an underlying diffusive scattering (3).

Table 1
The parameters of the second SAXS maximum (height I_{max}, center S_{max}, and integral width Δ_S) found by a least-squares fit according to the formula (3) and Bragg distances $d = (S_{max})^{-1}$ for MF-4SK wet membranes treated with ethylene glycol for various periods of time τ

τ (min)	I_{max} (rel.units)	S_{max} (nm^{-1})	Δ_S (nm^{-1})	d (nm)
0 (untreated)	2.65	0.202	0.106	4.95
0.5	2.94	0.182	0.124	5.49
2	3.85	0.162	0.129	6.17
9	4.50	0.154	0.124	6.49
30	5.24	0.147	0.125	6.80

maximum at $S \approx 0.2\ \mathrm{nm}^{-1}$ arises from the one-dimensional quasi periodicity in the direction normal to the polymeric bilayers and a shift of this maximum to smaller scattering angles denotes an increase in the quasi period of these bilayers.

In order to analyze this one-dimensional layered nanostructure of MF-4SK membranes and its alteration under the action of ethylene glycol in a quantitative manner we applied the paracrystalline X-ray diffraction theory [38,40–42], i.e. the diffraction theory accounting for the lattice distortions of the second kind.

Let $\rho(x)$ be the projection of an electron density of such a layered structure to the axis x normal to the polymer bilayer planes, $\rho_o(x)$, the same projection of an electron density of one bilayer and ρ_a, an electron density of aqueous layers separating adjacent bilayers. We assume that all bilayers have the same $\rho_o(x)$, and paracrystalline lattice distortions arise from a variation of the thickness of the aqueous layers. For such a structure model the intensity function corresponding to $\Delta\rho(x) = \rho(x) - \rho_a$ is given on the relative scale by

$$I(S) = [\Im\{\Delta\rho(x)\}]^2 = \{f^2(S)Z(S)\} * V(S), \quad (4)$$

where $\Im$, the symbol of the Fourier transform; $f(S) = \Im\{\Delta\rho_o(x)\}$, the scattering amplitude (the structure factor) for a single bilayer with electron density profile $\Delta\rho_o(x) = \rho_o(x) - \rho_a$; $Z(S)$, the interference function (lattice factor); $V(S)$, the shape factor; $*$, the symbol of the convolution operation.

We assume that the layered structure contains many

Table 2
The water content W (weight%) in MF-4SK membranes and the quantum yield $\Phi(AO_2)$ of anthracene photo-oxidation catalyzed by TPP immobilized in MF-4SK membranes for membranes treated with ethylene glycol for various periods of time τ

τ (min)	W (wt%)	$\Phi(AO_2).(10^{-5})$
0 (untreated)	22	5.2
0.5	26	12.3
2.0	31	10.6
8.0	–	12.2
9.0	35	12.7
30	31	9.1

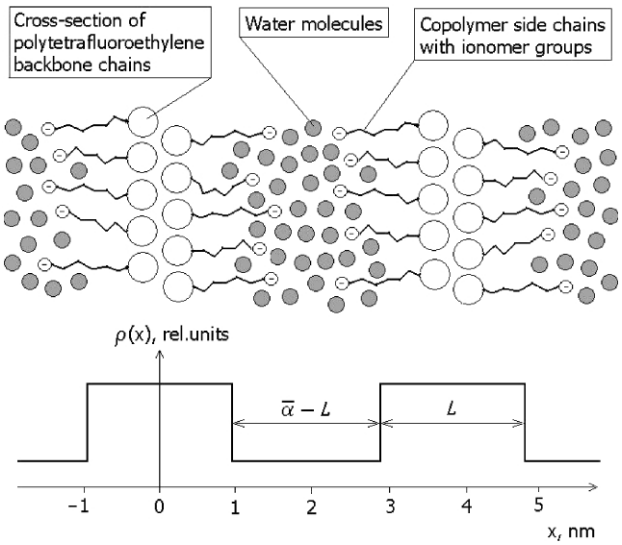

Fig. 10. A cross-section of the layered structure model for ionic clusters in a perfluorinated sulfocationic membrane and its schematic electron density distribution $\rho(x)$.

layers and the thickness W of this structure is large. The shape factor $V(S)$ is centered at $S = 0$ and has a width approximately equal to $(W)^{-1}$ [40,41]. So for large W the shape factor is pointlike with respect to $Z(S)$ and $V(S)$ does not influence the SAXS maximum. Then instead of (4) one gets

$$I(S) = f^2(S)Z(S) \tag{5}$$

In SAXS study we can approximate the profile of one bilayer $\rho_o(x)$ with the step function of the width L as shown in Fig. 10. For such $\rho_o(x)$

$$f(S) = \frac{\sin(\pi LS)}{\pi S} \tag{6}$$

The interference function $Z(S)$ in our case can be written [41] as

$$Z(S) = \frac{1 - |F(S)|^2}{1 - 2|F(S)|\cos(2\pi S\bar{\alpha}) + |F(S)|^2} \tag{7}$$

where $F(S)$ is the Fourier transform of the distance distribution function H_1 for the centers of adjacent bilayers

$$F(S) = \Im[H_1(x)] \tag{8}$$

and $\bar{\alpha}$, is the average distance between the centers of such bilayers.

We assume as in [40,41] that H_1 follows the normal Gaussian law with mean square deviation σ

$$H_1(x) = \frac{1}{\sigma\sqrt{2\pi}}\exp\left(-\frac{(x+\bar{\alpha})^2}{2\sigma^2}\right) \tag{9}$$

and

$$|F(S)| = \exp[-2(\pi S\sigma)^2] \tag{10}$$

After the substitution of (6),(7),(10) in (5) and introduction of a scaling factor A one gets

$$I(S) = \frac{A\sin^2(\pi LS)}{(\pi S)^2} \times \frac{1 - [\exp(-2(\pi S\sigma)^2)]^2}{1 - 2\exp(-2(\pi S\sigma)^2)\cos(2\pi S\bar{\alpha}) + [\exp(-2(\pi S\sigma)^2)]^2} \tag{11}$$

The experimental intensity was multiplied with the Lorenz correction factor S^2 [43] and then this corrected intensity was least-squares fitted with the expression (11) for $0.06\ \text{nm}^{-1} < S < 0.36\ \text{nm}^{-1}$ with A, L, $\bar{\alpha}$ and σ as variables. Examples of these fits are shown in Fig. 11. Parameters L, $\bar{\alpha}$, σ determined for membranes before and after the treatment with ethylene glycol are given in Table 3. Note that the values of $\bar{\alpha}$ derived by the paracrystalline

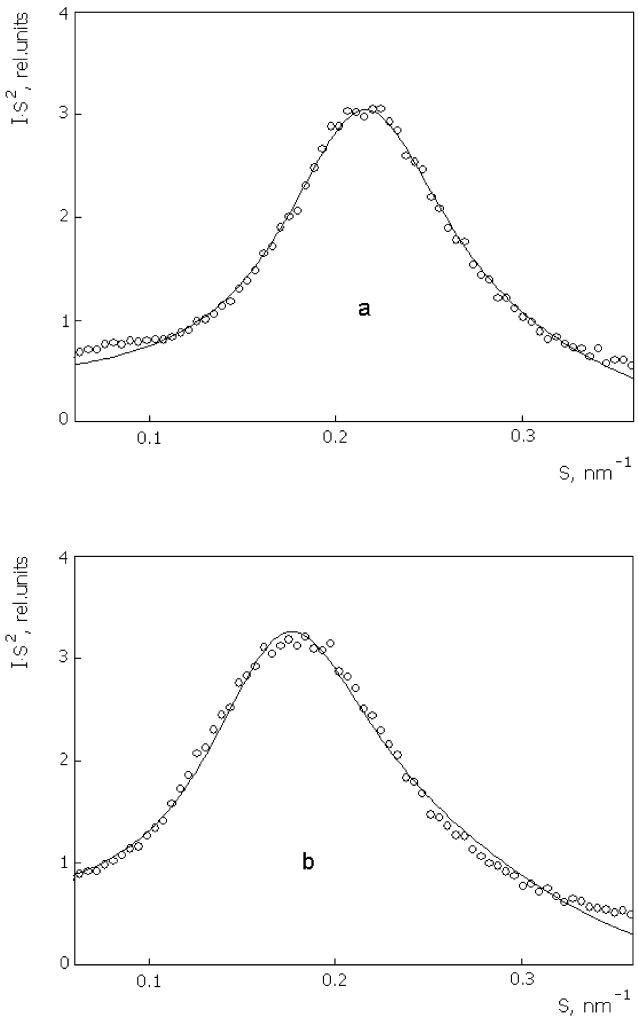

Fig. 11. The Lorentz corrected experimental SAXS data (circles) and its least-squares fits (solid lines) with the expression (11) for MF-4SK wet membranes before (a) and after (b) the treatment with ethylene glycol for 9 min.

Table 3
The parameters found by a least-squares fit for the Lorentz corrected experimental intensity $I(S)S^2$ with the expression (11) for MF-4SK wet membranes treated with ethylene glycol for various periods of time τ

τ (min)	L (nm)	σ (nm)	$\bar{\alpha}$ (nm)	$\sigma/\bar{\alpha}$	$\bar{\alpha} - L$ (nm)
0 (untreated)	2.09	1.29	4.08	0.316	1.99
0.5	2.10	1.48	4.19	0.353	2.09
2	2.18	1.66	4.49	0.370	2.31
9	2.20	1.78	4.71	0.378	2.51
30	2.21	1.87	4.77	0.392	2.56

approach (Table 3) are essentially less than the Bragg distances (Table 1).

For all the membranes the fits with (11) gave almost the same values of bilayer thickness L (Table 3). It was 2.09 nm for untreated membranes and it increased up to 2.21 nm (i.e. for only 6%) for membranes treated for 30 min with ethylene glycol. This shows that ethylene glycol had only minor effect on the structure of polymeric bilayers in the layered structure of ionic clusters in MF-4SK membranes. This conclusion is in accordance with the results of our WAXS study of ethylene glycol effect on MF-4SK membranes.

The average spacing $\bar{\alpha}$ and its mean square deviation σ considerably increased after membranes were treated with ethylene glycol (Table 3). This means that ethylene glycol essentially enlarged the interbilayer distance and variation of this distance in MF-4SK membranes. The values of $\sigma/\bar{\alpha}$ (Table 3) show that disorder in the layered nanostructure of perfluorinated sulfocationic membranes is very high and it increases even more under the action of ethylene glycol. One can also notice the values of parameters in Table 3 allow partial overlapping of bilayers. This is very likely a result of the use of simplified symmetric distance distribution function $H_1(x)$. This overlapping does not seem to be very significant as it does not exceed 2–3% of the bilayer mass for all the membranes studied.

We can assess the width of the aqueous layers (ionic channels) in MF-4SK membranes as the difference of the average spacing $\bar{\alpha}$ and the polymeric bilayer thickness L (Table 3). We get the thickness of this aqueous layers to be about 2 nm in untreated membrane and about 2.5 nm in membranes treated with ethylene glycol for 9–30 min. Surely these values are overestimated because they were determined by the calculations with a step function profile $\rho_o(x)$. The ratio of 2.5 nm/2 nm = 1.25 may be considered as the ratio of the water content in membranes treated with ethylene glycol and in untreated membranes. This ratio reasonably agrees with the mean ratio of the water content in these membranes determined on the basis of the gravimetric measurements (Table 2) which equals to 33%/22% = 1.5.

4. Conclusions

The SAXS and WAXS studies showed that soaking of perfluorinated sulfocationic membranes MF-4SK in ethylene glycol at 110 °C caused fast and stable alterations of their nanostructure while their molecular structure remained essentially unchanged. The SAXS data processed according to the paracrystalline diffraction theory showed that such a treatment of MF-4SK membranes increased the thickness of the aqueous layers (ionic channels) in ionic clusters of these membranes. This conclusion agrees with the higher water content in membranes treated with ethylene glycol. The growth of the quantum yield of anthracene photo-oxidation catalyzed by tetraphenylporphyrin (TPP) immobilized on MF-4SK membranes treated with ethylene glycol can be explained by a higher TPP accessibility for a substrate due to the broadened ionic channels in such membranes.

Acknowledgements

We acknowledge the research workers of the SAXS laboratory from the Institute of crystallography of the Russian Academy of Sciences for passing us the computation program of collimation correction. This work was financially supported by the International Scientific-Technical Centre (ISTC), Grant No. 1592.

References

[1] Timashev SF. Physical chemistry of membrane processes. Chichester: Ellis Horwood; 1991.
[2] Appleby AJ, Foulkes FR. Fuel cell handbook. New York: Van Nostrand Reinhold; 1989.
[3] Ciureanu M, Roberge R. J Phys Chem B 2001;105:3531–9.
[4] Huang H, Dasgupta PK, Genfa Z. Anal Chem 1996;68:2062–6.
[5] Richardson JN, Dyer AL, Stegemiller ML, Zudans I, Seliskar CJ, Heineman WR. Anal Chem 2002;74:3330–5.
[6] Wang J, Musameh M, Lin Y. J Am Chem Soc 2003;125:2408–9.
[7] Galeska I, Chattopadhyay D, Moussy F, Papadimitrakopoulos F. Biomacromolecules 2000;1:202–7.
[8] Allain LR, Canada TA, Xue Z. Anal Chem 2001;73:4592–8.
[9] Allain LR, Xue Z. Anal Chem 2000;72:1078–83.
[10] Khramov AN, Collinson MM. Anal Chem 2000;72:2943–8.
[11] Guo ZX, Sun N, Li J, Dai L, Zhu D. Langmuir 2002;18:9017–21.
[12] Solovieva AB, Lukashova EA, Vorobiev AV, Timashev SF. React Polym 1992;16:9–17.
[13] Liu P, Bandara J, Lin Y, Elgin D, Allard LF, Sun YP. Langmuir 2002; 18:10398–401.
[14] Yagi M, Sukegawa N, Kasamastu M, Kaneko M. J Phys Chem B 1999;103:2151–4.
[15] Kiwi J, Denisov N, Gak Y, Ovanesyan N, Buffat PA, Suvorova E, Gostev F, Titov A, Sarkisov O, Albers P, Nadtochenko V. Langmuir 2002;18:9054–66.
[16] Roche EJ, Pineri M, Duplessix R, Levelut AM. J Polym Sci Polym Phys Ed 1981;19:1–11.
[17] Gierke TD, Munn GE, Wilson FC. J Polym Sci Polym Phys Ed 1981; 19:1687–704.

[18] Fujimura M, Hashimoto T, Kawai H. Macromolecules 1981;14: 1309–15.
[19] Fujimura M, Hashimoto T, Kawai H. Macromolecules 1982;15: 136–44.
[20] Ozerin AN, Rebrov AV, Yakunin AN, Bogovtseva LP, Timashov SF, Bakeev NF. Vysokomolekulyarnie soedineniya 1986;A28:254–9. in Russian.
[21] Ozerin AN, Rebrov AV, Yakunin AN, Bessonova NP, Dreiman NA, Sokolov LF, Bakeev NF. Vysokomolekulyarnie soedineniya 1986; A28:2303–7. in Russian.
[22] Halim J, Buchi FN, Haas O, Stamm M, Scherer GG. Electrochim Acta 1994;19:1303–7.
[23] Halim J, Scherer GG. Macromol Chem Phys 1994;195:3783–8.
[24] Haubold HG, Vad Th, Jungbluth H, Hiller P. Electrochim Acta 2001; 46:1559–63.
[25] Manley DS, Williamson DL, Noble RD, Koval CA. Chem Mater 1996;8:2595–600.
[26] Litt MH. Polym Prepr 1997;38:80–1.
[27] Gebel G, Lambard J. Macromolecules 1997;30:7914–20.
[28] Elliott JA, Hanna S, Elliott AMS, Cooley GE. Macromolecules 2000; 33:4161–71.
[29] James PJ, Elliott JA, Newton JM, Elliott AMS, Hanna S, Miles MJ. J Mater Sci 2000;35:5111–9.
[30] Elliott JA, Hanna S, Elliott AMS, Cooley GE. Polymer 2001;42: 2251–3.
[31] Rubatat L, Rollet AL, Gebel G, Diat O. Macromolecules 2002;35: 4050–5.
[32] Rollet AL, Diat O, Gebel G. J Phys Chem 2002;106:3033–6.
[33] Barbi V, Funari SS, Gehrke R, Scharnagl N, Stribeck N. Polymer. In press.
[34] Franks A. Br J Appl Phys 1958;9:349–52.
[35] Cheremukina GA, Chernenko SP, Ivanov AB, Pashekhonov VD, Smykov LP, Zanevsky YuV. Isotopenpraxis 1990;26:547–9.
[36] Shedrin BM, Feigin LA. Kristallografia 1966;11:159–63. in Russian.
[37] Starkweather HW. Macromolecules 1982;15:320–3.
[38] Feigin LA, Svergun DI. Structure analysis by small-angle X-ray and neutron scattering. New York: Plenum Press; 1987.
[39] Rebrov AV, Ozerin AN, Svergun DI, Bobrova LP, Bakeev NF. Vysokomolekulyarnie soedineniya 1990;A32:1593–1598. in Russian.
[40] Hosemann R, Bagchi SN. Direct analysis of diffraction by matter. Amsterdam: Noth-Holland; 1962.
[41] Vainshtein BK. Diffraction of X-rays by chain molecules. Amsterdam: Elsevier; 1966.
[42] Cryst B. J Polym Sci 1973;11:635–61.
[43] Cryst B, Worthington CR. J Appl Cryst 1980;13:585–90.